Revista de la Asociación Española de Materiales Compuestos
MATERIALES COMPUESTOS
http://revista.aemac.org

http://revista.aemac.org/
Vol 1, nº 1, pág. 170-174

ISSN: 2531-0739

M. Iturrondobeitia[a], J.Ibarretxe[a], R. Fernadez Martinez[a], P.Jimbert[a], A.Okariz[a], V. Srot[b], P.A. van Aken[b], T. Guraya[a]

[a] eMERes, Escuela de Ingenieria de Bilbao, Universidad del País Vasco, 48013, Bilbao
[b] Stuttgart Center for Electron Microscopy, Max Planck Institute for Solid State Research, Heisenbergstr. 1, 70569 Stuttgart, Germany

Tomografía TEM de nanocomposites de Ácido poliláctico/arcillas para la definición de la relación entre el procesado, la microestructura y las propiedades

RESUMEN

Historia del artículo:
Recibido 5 de Mayo 2017
En la versión revisada 5 de Mayo 2017
Aceptado 31 de Mayo 2017
Accesible online 21 de Junio 2017

Palabras clave:
Tomografía
Segmentación
Microestructura
Bionanocompuestos
Propiedasdes mecánicas

Las propiedades físico-químicas de los nanocomposites poliméricos (como los sistemas de polímero/arcillas) dependen de las propiedades del polímero y del refuerzo, de la interfase entre el refuerzo y la matriz, y del tamaño, forma, orientación y distribución del refuerzo. Por lo tanto, la caracterización exhaustiva de la morfología de estos materiales posibilita una mejor comprensión de su comportamiento y en consecuencia una mejora de las herramientas de diseño del producto final. En función de la morfología del refuerzo dentro de la matriz a veces la caracterización exhaustiva requiere incluir las tres dimensiones. La tomografía electrónica (ET) permite una caracterización en detalle y en 3D de la microestructura de los composites de ácido poliláctico (PLA) / arcillas. Este tipo de análisis provee información determinante de la morfología (como la orientación, distribución y dmensiones de las partículas) no obtenible por medio del análisis cualitativo o cuantitativo de imágenes TEM convencionales (2D), ni por medio de técnicas de caracterización en masa como la difracción de rayos X.

En el presente trabajo se analizan muestras de PLA/Cloisite 30B obtenidas por extrusión en varias condiciones de procesado (velocidades de extrusión), que a su vez se reflejan en nanocomposites con distintos grados de exfoliación y dispersión de las arcillas, y por tanto en nanocomposites con distintas propiedades finales. En este trabajo se analiza el comportamiento de los nanocomposites determinando las relaciones existentes entre la información de microestructura obtenida por tomografía, el procesado y las propiedades finales observadas.

Quantitative TEM tomography of Poly lactic acid/clay nanocomposites for a better comprehension of processing-microstructure-properties relationship

ABSTRACT

Keywords:
Tomography
Segmentation
Microstructure
Bionanocomposites
Mechanical properties

The physicochemical properties of polymer nanocomposites (such as polymer/clay systems) are dependent on the properties of the polymer and filler, the reinforcement dimensionality, dispersion and orientation, and the nature of the interface between filler and matrix. Hence, thoroughly characterizing the morphology of those materials can lead to a better understanding of the behaviour of the final product and to improved design tools. The objective of performing TEM tomoghraphy (TEMT) on Poly lactic acid(PLA)/clay samples is to characterize their 3D microstructure, by obtaining the dispersion, distribution and orientation of the dimensions of the clays. This information cannot be elucidated from a qualitative TEM analysis or from conventional characterization techniques such as X-Ray diffraction.

To carry out this work, nanocomposites obtained by extruding a PLA matrix and Cloisite 30B clays are used. The nanocomposites are obtained by using different extrusion shear rates. Shear rate favours the exfoliation of the clay particles and their dispersion, leading to nanocomposites with different microstructures and properties. Then, quantitative TEMT is performed to all the nanocomposites and the resulting 3D quantitative characterization is used for the comprehension of the mechanical behaviour of the nanocomposites.

Autor de contacto: Maider Iturrondobeitia
e-mail: maider.iturrondobeitia@ehu.eus

1 Introduction

Poly (lactic acid) or PLA is one of the most used biodegradable and biocompatible polymers[1,2], but its range of application is still somewhat limited by several factors, notably due to its low thermal stability and limitted mechanical properties. In order to improve the properties, montmorillonite (organomodified) clays have been blended with the polymer. Mixing the polymer with clays at the nanoscale results in improved mechanical and functional properties with respect to the neat polymers or conventional composites[3] in those systems where there is an efficient interfacial interaction between matrices and organically modified layered silicates (OMLSs) [4-13]. These interactions are susceptible to the processing conditions.

The extent of clay platelet separation after integration with the (polymer) matrix (i.e. the degree of exfoliation) is a key parameter of the microstructure of laminar nanocomposites that has a significant effect on the final properties of the material[1,2]. Several techniques have been used to evaluate the clay disaggregation: transmission electron microscopy (TEM), X-ray diffraction (XRD) solid-state nuclear magnetic resonance (NMR) and atomic force microscopy (AFM) [14-17] . TEM is the only one of all these techniques that can provide a direct observation of the degree of exfoliation in the matrix. However, due to the projection nature of conventional (2D) bright-field (BF) TEM images, the orientation and dimensions of the clay objects cannot be directly and reliably measured (see Figure 1). This limitation can be overcome by means of electron tomography (ET), which has the capability to render microstructural features in three-dimensions (3D) at the nanometer scale[18,19].

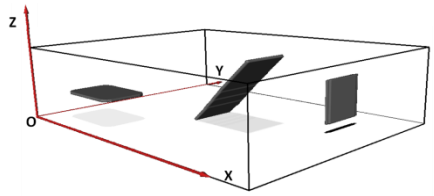

Figure 1. Changes in projected shape and contrast (grey level intensity) of laminar objects with different orientations.

The objective of performing quantitative transmission electron microscopy tomography (TEMT) on PLA/clay samples is to characterize their 3D microstructure. The dimensions, distribution and orientation of the clays will be obtained. Such a quantitative 3D characterization will offer a better understanding of the mechanical behavior of PLA/clay nanocomposites.

The accuracy of quantitative ET depends among other factor on the segmentation of the objects [20-23]. The most popular options are based on the threshold and watershed methods, but there are also other approaches based on advanced computationi [10]. Despite the existence of all these possibilities, to date none of them stands out as a generally applied segmentation method. Actually, manual segmentation still remains as the prevalent method of choice. In this regard, a simple, efficient and objective methodology to perform the segmentation that was previously reported[24,25] will be applied herein. An objective procedure is of great importance when the aim of the 3D quantification is to compare microstructures of different materials.

To date, several ET studies of clay based nanocomposites have been published, based on epoxy/clay latex/clay, PBSA/clay or EVA/clay [26-29]. However, Only Nawani et al. [29] showed an EVA/clay segmented 3D volume and none of them have used a quantitative characterization for the explanation of the properties of the material.

The aim and novelty of the current work is to perform and show in detail a 3D TEMT quantitative analysis of PLA/Closite30B nanocomposites and to use the microstructural parameters to understand the relationship between the processing conditions and the final mechanical properties.

2 Experimental

2.1 Materials

Natureworks® LLC polymer grade 3051D Poly (lactic acid) — provided by Cargill-Dow — was used for the samples. The material was received in pellets having a melt flow index of 9 g 10 min-1 (190 °C and 2.16 kg). Organically treated montmorillonite Cloisite 30B from Southern Clay Products (Gonzales, TX) was used as reinforcement.

The PLA/5wt % clay samples were prepared in a Brabender Plasticorder DSE 20/40D co-rotating twin-screw extruder at 190 °C and three different extrusion speeds: 120, 300 and 650 rpm. Before processing, the PLA was dried for 4 h at 80 °C and the clay for 12 h at 80 °C. The samples were also pre-dried for a injection moulding for 4 h at 80 °C, and A type specimens were injection moulded according to ISO 527 in a Sandretto OTTO 150 Tn injection moulding machine[30]. Neat PLA was also processed at the same conditions as reference.

2.2 Tomography

A Leica Ultracut UCT cryo-ultramicrotome stage was used to cut 130 nm thick slices from the middle and inner area of the A type injection molded samples of each nanocomposite.
The experimental tilt series was acquired in bright-field TEM (BF-TEM) mode using a Zeiss EM 912 Omega microscope operated at 120 kV. BF-TEM images were acquired at every 2° in the angular range of ± 70°. In this work, all the tomographic reconstructions were performed using the Simultaneous Iterative Reconstruction Technique (SIRT) available in commercial and free software packages. A threshold based segmentation was carried out following the methodology previously reported in [25].The quantified microstructural parameters are described in table 1 and were calculated using Fiji free software[31].

Table 1. Parameters measured from ET.

Parameter	Definition
Clay particles (ncp)	Number of objects per volume
Distances (D4)	Averaged distances between the centroids of the 4 nearest objects
3D Misalignment	Average of the angles between the axes of the main moment of inertia of the objects, calculated for every combination of two clays.
Length (Lcp) and thickness (dcp)	Average of the maximum Feret diameter of each object. Average of the minimum Feret diameter of each object

2.3 Tensile test

The elastic modulus (E) was measured in a conventional mechanical testing machine, Hounsfield H25K5, at a speed of 10 mm·min^{-1}.

3 Results and discussion

The 3D TEM reconstructed volumes for the PLA/Cloisite 30B bionanocomposites processed at diferent conditions are shown in Figure 2. In the reconstructed volumes the draker pixels belong to the clay particles and the brighter ones to the background, the polymer.

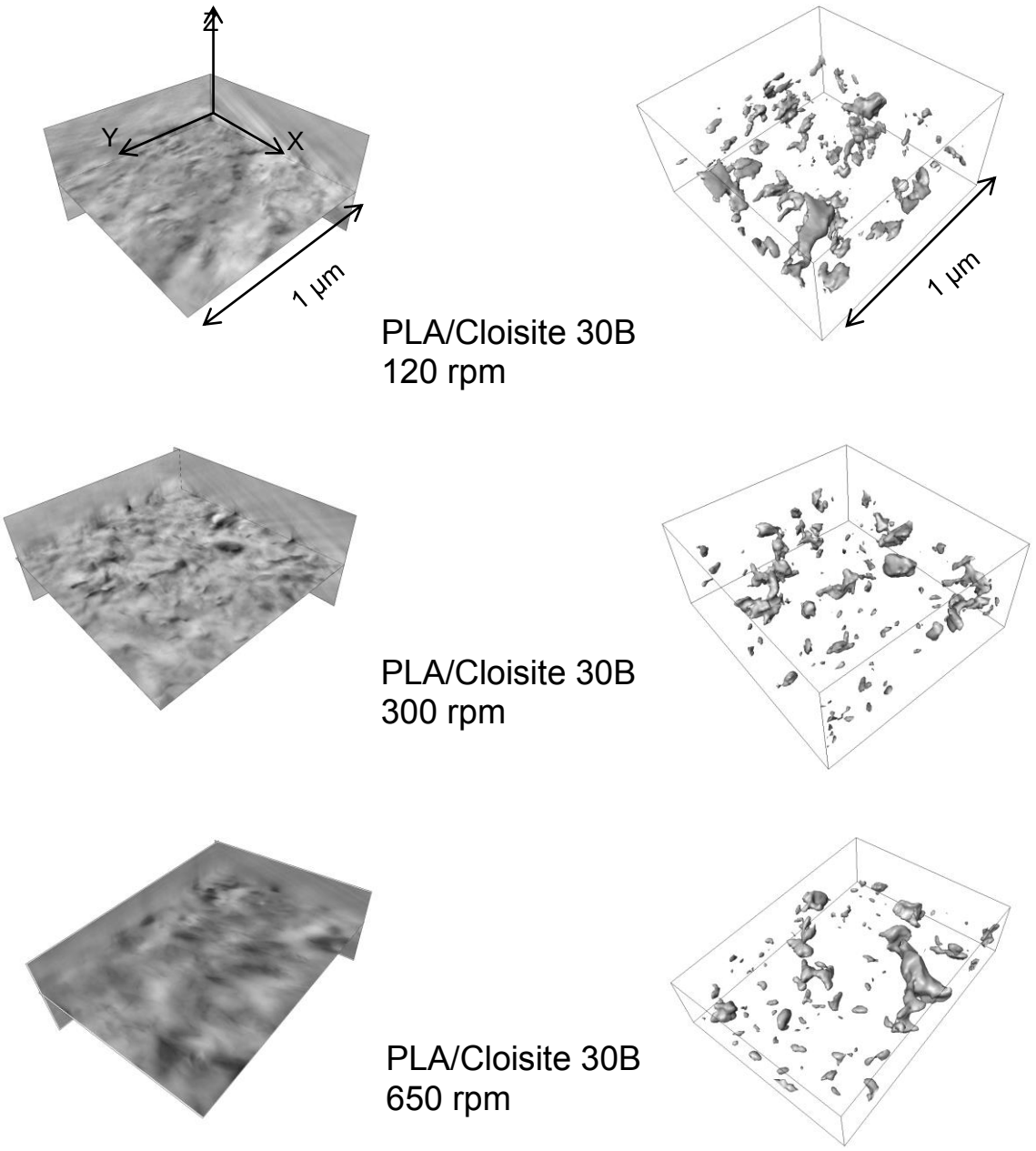

Figura 2. 3D reconstructed volumes (left) and their correspondng segmented volumes (right) for each nanocomposite.

Prior to the quantification of the microstructural parameters described in Table 1, a segmentation where the clay particles are separated from thebackground is required. The results obtained from this process are shown in Figure 2. It can be observed that the number of clay particles increases with the increasing shear rate. However, for a more detailed analysis, microstructural parameters are quantified and the results are summerized in the folowing Table 2.

Table 2. Results obtained from the quantification.

	ncp/V ·109(nm-3)	Lcp (nm)	dcp (nm)	D4 (nm)	3D Misalig. (º)
PLA/30B 120	243	92±90	32±20	129±30	47±20
PLA/30B 300	365	68±70	26±30	100±20	55±20
PLA/30B 650	391	58±70	25±40	125±30	53 ±20

The 3D analysis shows that the number of clay particles tends to increase with increasing extrusion speed. This increase in the number of particles can be attributed to the disaggregation of the clay sheets or to the fracture of the silicate layers.

The evolution of the thickness and the length for the nanocomposites follow the invers of trend described for the ncp. The thicknesses measured from the TEMT reconstruction are high compared to those found in the literature, measured from XRD. These dissimilarities are probably due to a combination of factors. First, the segmented 3D objects must be distorted due to the effect of the missing wedge. Second, the proposed segmentation methodology will probably not result in extremely well resolved segmented objects. Finally, the curved, flake-like shape of the clays renders the automated measurement of the thickness rather difficult, whereas such measurement is accurate enough in the case of flat layers. The trend of the distances is inverse to that of the number of clay particles. Since the amount of clays is the same in all the samples, the D'4 value is an indicator of the dispersion. Therefore an optimum in the dispersion is detected for the nanocomposite processed at 300 rpm. The misalignment degree increases when the extrusion speed is increased from 120 rpm to 300 rpm, although for a further increase in the extrusion speed it remains almost constant.

The modulus of the PLA, 2700 MPa does not vary with the processing conditions. By extruding PLA with Cloisite30B clay particles at 120 rpm an increment of the modulus of 24 % is achieved. By increasing the extrusion speed up to 300 rpm the modulus is improved in a 40 %. Conversely, another additional increment in the extrusion speed (650 rpm) only induces an increment of 24 %.

To understand the relationship between the processing conditions and the elastic modulus the microstructural parameters are used. The ncp parameter indicates a larger amount of present clay particles as the extrusion speed increases. This fact can be atributed on the one hand to a better exfoliation degree or on the other hand to a breakage of the clay particles. dcp and Lcp parameters can be helpfull to uncover the relationship. The larger the Lcp and lower dcp, the higher the exfoliation degree and thus the more effective reinforcing effect is expected and therefore an optimum improvememt of the elastic modulus. In this regard, the nanocomposite extruded at 120 rpm has the higher Lcp and dc values which indicates a low exfolation degree. As the extrusion speed increases the dcp decreases and so does the Lcp. This fact indicates a partial breakage of the clay particles as well as a higher exfoliation degree. However, by increasing the extrusion speed up to 650 rpm the dcp remains constant while the Lcp keeps on decreasing, which points towards an additional breakage of the clay particles instead of an improvement in the exfoliation degree, which turns into an ineffective reinforcing effect of the clay particles.

4 Conclusions

TEMT has been successfully applied to bio based polymer nanocomposites and has proven to be an effective tool for the 3D characterization of the microstructure. From the 3D characterization relevant microstructure describers have been computed and used to clarify the behavior of the reinforcing clay particles during the transformation process. Finally, from the characterization and the posterior analysis of the data, it has been concluded that the best compromise between the processing condition- exfoliation degree and breakage of the particles must be found in order to obtain an optimum nanocomposite with the best final properties. For this purpose microstructural describers such as the Lcp, dcp, D4 and ncp have proven to be helpful.

Acknowledgements

Financial support from the Basque Government (GV-IT-303-10 and S-PE11UN047) and Biscay Regional Government (DFV 6-12-TK-2010-25); The European Union Seventh Framework Programme under Grant Agreement 312483 ESTEEM2 (Integrated Infrastructure Initiative–I3); Leartiker.

References

1. Madhavan, N.; Nimisha Rajendran, N.; Rojan Pappy, J.; Bioresource technology. 2010, 101, 8493-8501.

2. Gupta, A.P.; Kumar, V.; European Polymer Journal. 2007, 43, 4053-4074.

3. Ray, S.S.; Okamoto, M.; Progress in Polymer Science. 2003, 28, 1539-1641.

4. Nieddu, E.; Mazzucco, L.; Gentile, P.; Benko, T.; Mandrile, R.; Ciardelli, G.; Reactive & Functional Polymers. 2009, 69,371-379.

5. Henriette, M.C.; Food Research International. 2009, 42-1240-1253.

6. Gámez-Pérez, J.; Nascimiento, L.; Bou, J.J.; Franco-Urquiza, E.; Santana, O.O.; Carrasco, F.; Maspoch, M.L.; Journal of Applied Polymer Science. 2011, 120,896-905.

7. Pavlidou, S., Papaspyrides, C.D; Progress in Polymer Science. 2008 33 119-1198.

8. Fukushima, K., Tabuani, D., Camino, G.; Material Science and Engineering C. 2012 32 1790-1795.

9. Ojijo, V., Ray, S.S.; Progress in Polymer Science. 2013 38, 1543-1589.

10. Najafi, N., Heuzey, M.C., Carreau, P.J.; Composites Science and Technology. 2012 72 608-615.

11. Wei, P., Bocchini, S., Camino, G.; European Polymer Journal. 2013 40 932-939.

12. Zhu, J., wilkie, C.A.; Polym Int. 2002 49 1158-1163.

13. Paul, M.A., Alexandre, M., Degée, P., Henrist, C., Rulmont, A., Dubois, P.; Polymer. 2003 44 443-450.

14. Ratinak, K.R.; Gilbert, G.R.; Ye, L.; Jones, A.S.; Ringer, S.P.; Polymer. 2006 47 6337-6361.

15. Ray, S.S.; Okamoto, M.; Fujimoto, Y.; Ogami, A.; Ueda, K.; Polymer. 2003 44 6633-6646.

16. Araujo, A.; Botelho, G.; Oliveira, M.; Machado, A.V.; Applied Clay Science. 2014 88-89 144-150.

17. Gélinas, V.; Vidal, D.; Powder Technology. 2010 203 254-264.

18. Midgley, P.A.; Weyland, M.; Ultramicroscopy. 2003 96 413-431.

19. Arslen, I.; Yate, T.J.V.; Browing, N.D.; Midgley, P.A.; Science. 2005 309 2195-2198.

20. Xu, B.; Quian Zeng, Q.; Somg, Y.; Shangguan, Y.; Polymer. 2006 47 2904-2910.

21. Lu, C.; Mai, Y.W.; Physical Review letters. 2005 95 088303.

22. Wang, X.Y.; Lockwood, R.; Malac, M.; Furukawa, H.; Li, P.; Meldrum, A.; Ultramiscroscopy. 2012 113 96-105.

23. Fernandez, J.J.; Micron. 2012 43 1010-1030.

24. Iturrondobeitia, M.; Ibarretxe, J.; Okariz, A.; Fernandez-Martinez, R.; Jimbert, P.; Guraya, T.; Srot, V.; Bussman, B.; van Aken, P.A.; AIP Conference proceedings. 2015 1653 020047-1-020047-7.

25. Iturrondobeitia, M.; Ibarretxe, J.; Okariz, A..; Guraya, T.; Srot, V.; Bussman, B.; van Aken, P.A.; Journal of applied polymer science. 2017 134-15.

26. Drummy, L.F.; Wang, Y.C.; Schoenmekers, R.; May, K.; Jackson, M.; Koener, H.; Farmer, B.L.; Mauryama, B.; Vaia, R.A.; macromolecules. 2008 41 2135-2143.

27. Negrete-Herrera, N.; Putaux, J.L.; David, L.; Haas, F.; Bourgeat-Lami, E.; Macromolecular Rapid communications. 2007 28 1567-1573.

28. Ray, S.S.; Macromolecular Materials and Engineering. 2009 294 281-286.

29. Nawani, P.; Burger, C.; Rong, B.; Chu, B.; Hsiao, B.S.; Tsou, A.H.; Polymer. 2010 51 5255-5266.

30. Iturrondobeitia, M.; Ibarretxe, J.; Okariz, A..;Zaldua, A.M.; Guraya, T.; Journal of Applied Polymer Science. 2014 131-18.

31. http://www.fiji.com . Schindelin J.; Arganda-carreras, I.; Frise, E.; Nature Methods. 2012 9 676-682. Ridler, T.W.; Calvard, S.; Picture thresholding using an iterative selection method, IEEE Trans. System, Man and Cybernetics. 1978 SMC-8 630-632.